

Article

# The Exploration and Analysis of the Magnetic Relaxation Behavior in Three Isostructural Cyano-Bridged 3d–4f Linear Heterotrinnuclear Compounds

Xia Xiong <sup>1</sup>, Yangyu Liu <sup>1</sup>, Shan Li <sup>1</sup>, Anqi Xue <sup>1</sup>, Juan Wang <sup>1</sup>, Chi Zhang <sup>1</sup>, Wenhua Zhu <sup>1,\*</sup>   
and Haoling Sun <sup>2,\*</sup>

<sup>1</sup> Hubei Collaborative Innovation Center for Advanced Organic Chemical Materials, Ministry-of-Education Key Laboratory for the Synthesis and Application of Organic Functional Molecules, College of Chemistry and Chemical Engineering, Hubei University, Wuhan 430062, China; xx1507126@163.com (X.X.); m17683724663@163.com (Y.L.); 15927404995@163.com (S.L.); 15071140143@163.com (A.X.); wangjuan\_hd@163.com (J.W.); zhangc\_zc@hubu.edu.cn (C.Z.)

<sup>2</sup> Department of Chemistry and Beijing Key Laboratory of Energy Conversion and Storage Materials, Beijing Normal University, Beijing 100875, China

\* Correspondence: zhuwenhua@pku.org.cn (W.Z.); haolingsun@bnu.edu.cn (H.S.);  
Tel.: +86-27-8866-2747 (W.Z.)

Received: 23 January 2018; Accepted: 20 March 2018; Published: 22 March 2018



**Abstract:** Three isostructural cyano-bridged 3d–4f linear heterotrinnuclear compounds,  $(\text{H}_2\text{O})_4\{\text{Ln}[\text{TM}(\text{CN})_5(\text{CNH}_{0.5})]_2(\text{HMPA})_4\}$  (Ln =  $\text{Y}^{\text{III}}$ , TM =  $[\text{Fe}^{\text{III}}]_{\text{LS}}$  (**1**); Ln =  $\text{Dy}^{\text{III}}$ , TM =  $[\text{Fe}^{\text{III}}]_{\text{LS}}$  (**2**); Ln =  $\text{Dy}^{\text{III}}$ , TM =  $\text{Co}^{\text{III}}$  (**3**)), have been synthesized and characterized by single-crystal X-ray diffraction. Due to the steric effect of the HMPA ligands, the central lanthanide ions in these compounds possess a low coordination number, six-coordinate, exhibiting a coordination geometry of an axially elongated octahedron with a perfect  $D_{4h}$  symmetry. Four HMPA ligands situate in the equatorial plane around the central lanthanide ions, and two  $[\text{TM}(\text{CN})_5(\text{CNH}_{0.5})]^{2.5-}$  entities occupy the apical positions to form a cyano-bridged 3d–4f linear heterotrinnuclear structure. The static magnetic analysis of the three compounds indicated a paramagnetic behavior of compounds **1** and **3**, and possible small magnetic interactions between the intramolecular  $\text{Dy}^{\text{III}}$  and  $[\text{Fe}^{\text{III}}]_{\text{LS}}$  ions in compound **2**. Under zero dc field, the ac magnetic measurements on **2** and **3** revealed the in-phase component ( $\chi'$ ) of the ac susceptibility without frequency dependence and silent out-of-phase component ( $\chi''$ ), which was attributed to the QTM effect induced by the coordination geometry of an axially elongated octahedron for the  $\text{Dy}^{\text{III}}$  ion. Even under a 1 kOe applied dc field, the  $\chi''$  components of **2** were revealed frequency dependence without peaks above 2 K. And under a 2 kOe and 3 kOe dc field, the  $\chi''$  components of **3** exhibited weak frequency dependence below 4 K with the absence of well-shaped peaks, which confirmed the poor single-ion magnetic relaxation behavior of the six-coordinate  $\text{Dy}^{\text{III}}$  ion excluding any influence from the neighboring  $[\text{Fe}^{\text{III}}]_{\text{LS}}$  ions as that in the analogue **2**.

**Keywords:** single-molecule magnets; single-ion magnets; lanthanide; coordination geometry

## 1. Introduction

With the rapid development of information technology, the current data storage materials are facing the limit of storage density and become unable to meet the growing needs of the future, thus the development of new high-density information storage materials have been paid more and more

attention [1]. Because of the magnetic bi-stability under the blocking temperature ( $T_B$ ), single-molecule magnets (SMMs) are expected to realize high-density information storage at the single-molecule level. SMMs or single-ion magnets (SIMs) involving lanthanide ions have been extensively developed since 2003 [2] due to the intrinsic magnetic anisotropy originating from the strong spin-orbit coupling of most lanthanide ions such as  $Tb^{III}$ ,  $Dy^{III}$ ,  $Ho^{III}$ ,  $Er^{III}$  [3–5]. Much higher effective energy barrier ( $U_{eff}$ ) and blocking temperature have been achieved in lanthanide-containing SMMs or SIMs than the first SMMs,  $Mn_{12}$  [6] and most of the later discovered transition metal-based SMMs.

It has been found that many factors could affect the performance of single molecule magnets. The coordination numbers, coordination geometry, dipolar interactions and the magnetic coupling from neighboring spin carriers have a significant impact on the magnetic relaxation behavior and the effect of quantum tunneling of the magnetization (QTM) in lanthanide-based SMMs [3,7]. The theoretical prediction suggests that an axial coordination geometry around a 4f ion with oblate electron densities such as  $Dy^{III}$  would possibly lead to a strong axial ligand field and to stabilize the maximal angular momentum projections [8,9]. An ideal axial symmetry to minimize the effect of transversal magnetic field and the induced QTM has been proposed to be achieved in an extreme case  $[DyO]^+$ , which is hardly available in the experiments [10]. The alternative approaches are to build axially high-symmetric  $Dy^{III}$ -containing compounds or low-symmetric cases with an especially short Dy–O bond to approach the theoretical limit of the effective energy barrier and the blocking temperature in lanthanide-based SMMs [11]. A growing number of excellent experimental results have confirmed the feasibility of these strategies. The examples are widely distributed in systems such as the widely studied square antiprismatic ( $D_{4d}$ ) [12], the later developed pentagonal bipyramidal ( $D_{5h}$ ) [13–17], the promising metallocenium [18,19], and the lanthanide alkoxide complexes [20]. Owing to the coordination ability of the sterically hindered ligands and the difficulty of controlling the coordination orientation, the low-coordinate lanthanide compounds with an axial symmetry are more difficult to obtain. Several reported cases include the nearly linear 2-coordinate ( $D_{\infty h}$ ) [21], the equatorially coordinated triangle ( $C_3$ ) [22], the trigonal-pyramidal (pseudo- $C_3$ ) [23], the five-coordinate [24], and the six-coordinate complexes [9,13,20,25–41].

In particular, it is relatively difficult to acquire strong uniaxial anisotropy in six-coordinate lanthanide compounds because the octahedral coordination geometry with uniform bond lengths is close to spherical symmetry. Considerable energy barriers under zero direct-current (dc) field have been discovered in octahedrally coordinated Dy-containing systems with one or two especially short Dy=C, Dy=N, Dy=O, and Dy=F bonds, such as a monometallic dysprosium(III) bis(methanediide) ( $U_{eff} = 813$  K) [9], a mononuclear six-coordinate dysprosium complex with trigonal-prismatic coordination geometry ( $U_{eff} = 190$  K) [25], a dysprosium thiolate cage ( $U_{eff} = 66$  K) [26], a  $Dy_5$  pyramid ( $U_{eff} = 528$  K) [20], a  $\{Dy_4K_2\}$  cluster ( $U_{eff} = 692$  K) [27], and the first dysprosium complex with a terminal fluoride ligand ( $U_{eff} = 760$  K) [28]. Relatively lower zero-field energy barriers have been acquired in some six-coordinate Dy-containing examples with a coordination geometry substantially deviated from the ideal octahedron ( $O_h$ ), such as a trigonal antiprism ( $U_{eff} = 11$  and  $14$  K) [29], a distorted trigonal prism ( $U_{eff} = 159$  K) [30] and an axially compressed octahedron (for the diluted sample,  $U_{eff} = 75$  K) [31]. Only field-induced energy barriers or even no relaxation parameters could be deduced from the alternating-current (ac) measurements in most of the six-coordinate complexes with more uniform bond lengths [13,32–41]. In spite of the above-mentioned six-coordinate dysprosium complexes, as far as we know, an example with a perfect  $D_{4h}$  symmetry has not been found yet [41]. Here we report the magnetic relaxation behavior in three isostructural cyano-bridged 3d–4f linear heterotrimeric compounds,  $(H_{2.5}O)_4\{Ln[TM(CN)_5(CNH_{0.5})_2(HMPA)_4]\}$  ( $Ln = Y^{III}$ ,  $TM = [Fe^{III}]_{LS}$  (1);  $Ln = Dy^{III}$ ,  $TM = [Fe^{III}]_{LS}$  (2);  $Ln = Dy^{III}$ ,  $TM = Co^{III}$  (3); HMPA = hexamethylphosphoramide), in which the central lanthanide ions exhibit an axially elongated octahedral coordination geometry with a perfect  $D_{4h}$  symmetry. Utilizing the  $[TM(CN)_6]^{3-}$  ( $TM = Fe^{III}$ ,  $Cr^{III}$ ) precursors as bridging or terminal ligands has been reported to successfully construct similar trimeric structure with another transition metal ion [42,43].

## 2. Results and Discussion

### 2.1. Crystal Structure of Compounds 1–3

The single-crystal X-ray diffraction analyses show that compounds 1–3 are isostructural and crystallize in the tetragonal space group  $I4/mmm$  (Table 1). Therefore, only the structure of compound 2 will be described in detail, with some important structural parameters of the other two compounds as comparison.

**Table 1.** Crystallographic data for the compounds 1–3.

	1	2	3
Empirical formula	$C_{36}H_{83}N_{24}P_4O_8YFe_2$	$C_{36}H_{83}N_{24}P_4O_8DyFe_2$	$C_{36}H_{83}N_{24}P_4O_8DyCo_2$
Formula weight	1304.75	1378.34	1384.50
Temperature/K	293(2)	293(2)	293(2)
Crystal system	Tetragonal	Tetragonal	Tetragonal
Space group	$I4/mmm$	$I4/mmm$	$I4/mmm$
<i>a</i> [Å]	12.9312(3)	12.9435(3)	12.8888(3)
<i>b</i> [Å]	12.9312(3)	12.9435(3)	12.8888(3)
<i>c</i> [Å]	19.4611(10)	19.5206(10)	19.3416(8)
$\alpha, \beta, \gamma$ [°]	90	90	90
Volume [Å <sup>3</sup> ]	3254.2(2)	3270.4(2)	3213.0(2)
<i>Z</i>	2	2	2
<i>D</i> <sub>c</sub> [g cm <sup>−3</sup> ]	1.332	1.400	1.431
$\mu$ (Mo <i>K</i> $\alpha$ ) [mm <sup>−1</sup> ]	1.482	1.726	1.821
Total reflections collected	16866	14604	16563
Uniq reflections ( <i>R</i> <sub>int</sub> )	1001(0.0633)	903(0.0661)	980(0.0517)
No. of refined parameters	144	146	144
<i>R</i> 1, <i>wR</i> 2 [ <i>I</i> ≥ 2 $\sigma$ ( <i>I</i> )]	0.0668, 0.1790	0.0449, 0.1250	0.0454, 0.1219
<i>R</i> 1, <i>wR</i> 2 (all data)	0.0840, 0.1932	0.0487, 0.1279	0.0492, 0.1242
Goodness of fit	1.113	1.142	1.155

As depicted in Figure 1a, compound 2 exhibits a linear trinuclear structure with two  $[Fe(CN)_5(CNH_{0.5})]^{2.5-}$  entities acting as terminal groups coordinating to a central Dy<sup>III</sup> ion. The entire molecule of compound 2 contains one Dy<sup>III</sup> ion, two  $[Fe(CN)_5(CNH_{0.5})]^{2.5-}$ , four HMPA and four hydronium ions (H<sub>2.5</sub>O)<sup>0.5+</sup>. Due to the addition of the HCl solution, the lattice water molecule, and the terminal cyano group of the  $[Fe(CN)_6]^{3-}$  entity along the *c* axis were both protonated by a half-occupied hydrogen atom. Similar hydronium ions as counter cations has recently been found in a charge-transfer (CT) salt of hexacyanidoferrate(II) [44]. And the hydrogen isocyanide (HNC) system has been discovered in the crystal lattice of similar “cyanometallic acids” [45]. The Dy<sup>III</sup> ion situates at the center of a nearly perfect octahedron (*D*<sub>4h</sub>), connected to the four oxygen atoms (O1, O1#3, O1#4, O1#5) from the HMPA ligands in the equatorial plane, and two N atoms (N1, N1#14) from the  $[Fe(CN)_5(CNH_{0.5})]^{2.5-}$  entities occupying the apical positions. The  $[Fe^{III}]_{LS}$  ion is six-coordinated by the cyano groups to form a nearly octahedral geometry. The four HMPA ligands and the four cyano groups in the equatorial plane both exhibit twofold disorder in the *ab* plane (Figure S1), while the HMPA ligands show another twofold disorder perpendicular to the *ab* plane. One set of disordered atoms are chosen to depict Figure 1a.

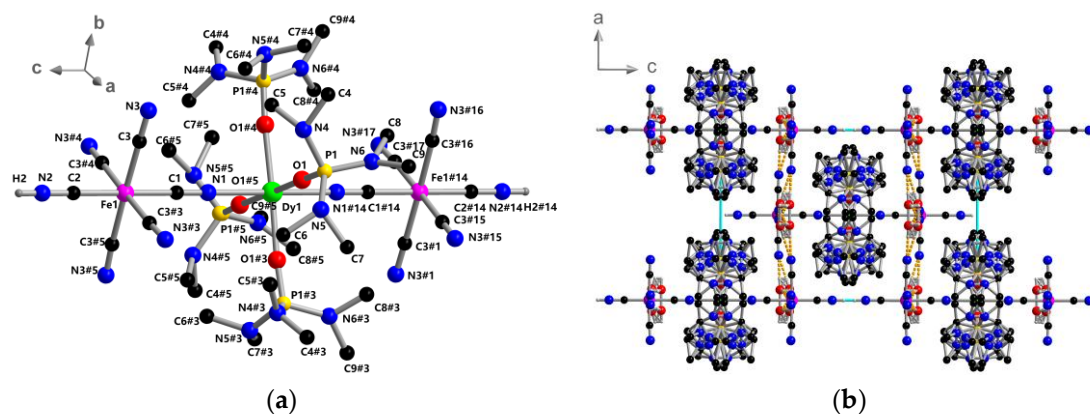


**Figure 1.** The molecular structure of compound **2**: (a) The coordination environment of the Dy(III) ions. Symmetry codes: #1  $-x, -y, -z$ ; #3  $y, -x, z$ ; #4  $-y, x, z$ ; #5  $-x, -y, z$ ; #14  $x, -y, -z$ ; #15  $y, -x, -z$ ; #16  $x, y, -z$ ; #17  $-y, x, -z$ ; (b) The packing diagram of compound **2** along the  $b$ -axis.

As listed in Table S3, for compound **2**, the axial N1–Dy–N1#14 angle is  $180^\circ$ . However, the four equatorial O–Dy–O angles,  $\angle O1\text{--}Dy1\text{--}O1\#3$ ,  $\angle O1\text{--}Dy1\text{--}O1\#4$ ,  $\angle O1\#3\text{--}Dy1\text{--}O1\#5$ ,  $\angle O1\#4\text{--}Dy1\text{--}O1\#5$ , are all  $89.98(44)^\circ$ , which are related by a fourfold axis. The O–Dy–N1 and O–Dy–N1#14 angles are  $89.20(70)^\circ$  and  $90.80(70)^\circ$ , respectively. The slight deviation of these O–Dy–O, O–Dy–N1 and O–Dy–N1#14 angles from strict  $90^\circ$  arises from the twofold disorder of the HMPA ligands on both sides of the equatorial plane. On the other hand, the axial C(1)–Fe(1)–C(2) angle is  $180^\circ$ , while  $\angle C1\text{--}Fe1\text{--}C3$  (or C3#3, C3#4, C3#5) and  $\angle C2\text{--}Fe1\text{--}C3$  (or C3#3, C3#4, C3#5) are respectively  $89.20(30)^\circ$  and  $90.80(30)^\circ$ . The departure from strict  $90^\circ$  of these bond angles around Fe1 originates from the different steric hindrance of the opposite side of the equatorial plane rather than the twofold disorder. The Dy<sup>III</sup> ion instead of the [Fe<sup>III</sup>]<sub>LS</sub> ions locate at the inversion center. For compounds **1–3**, the axial Ln–N distances of 2.353(11), 2.372(13) and 2.380(12) Å are slightly longer than the equatorial Ln–O distances of 2.208(11), 2.244(11) and 2.235(11) Å. As shown in Table S7, the coordination geometry of the Ln<sup>III</sup> ion was calculated by SHAPE 2.1 to be close to the octahedron geometry ( $O_h$ ), with the minimum CShM values of 0.131, 0.079, 0.105 respectively for compounds **1–3** [46,47]. The trivial CShM values deviated from an octahedron come from the disorder of the HMPA ligands and the axially elongated Ln–N bonds [41]. The axial TM–C1 and TM–C2 (TM = [Fe<sup>III</sup>]<sub>LS</sub> for **1** and **2**; TM = Co<sup>III</sup> for **3**) distances for compounds **1–3** are respectively 1.915(13), 1.904(15), 1.860(13) and 1.922(13), 1.906(14) Å, 1.869(13) Å, which are slightly shorter than the equatorial TM–C3 distances of 1.963(10), 1.946(10), 1.904(10) Å. Overall, the coordination geometry around the Ln<sup>III</sup> ions is an axially elongated octahedron, and that around the TM<sup>III</sup> ions is an axially compressed octahedron.

For compounds **1–3**, the intramolecular Ln $\cdots$ TM and TM $\cdots$ TM distances are respectively 5.4061, and 10.8122 Å (**1**), 5.4281 and 10.8562 Å (**2**), 5.3820 and 10.7640 Å (**3**). A packing diagram of **2** is shown in Figure 1b. The protonated hydrogen atom is involved in the hydrogen bond with the axial terminal cyano group of the [Fe(CN)<sub>5</sub>(CNH<sub>0.5</sub>)]<sup>2.5-</sup> entity from the neighboring linear trinuclear molecule. The super short N–H $\cdots$ N hydrogen bonds of 2.57 Å (**1**), 2.54 Å (**2**), 2.56 Å (**3**) are even stronger than that in H-cross-linked H<sub>3</sub>Co(CN)<sub>6</sub> (2.58 Å) [48]. As a result of the restraints of symmetry, the semi-occupied protonated hydrogen atoms appear on two equivalent positions in one N–H $\cdots$ N hydrogen bond [45]. The hydrogen atoms of the hydronium ions are involved in the hydrogen bonds with the equatorial terminal cyano groups of the neighboring [Fe(CN)<sub>5</sub>(CNH<sub>0.5</sub>)]<sup>2.5-</sup> entity. The shortest intermolecular TM $\cdots$ TM and Ln $\cdots$ Ln distances are 8.6489 and 12.9312 Å (**1**), 8.6644 and 12.9435 Å (**2**), 8.5776 Å and 12.888 Å (**3**), respectively, which indicates that the neighboring linear trinuclear molecules are relatively well isolated.

## 2.2. Magnetic Properties of Compounds 1–3

The phase purity of compounds 1–3 was confirmed by the good agreement of the PXRD data of the as-prepared samples with the corresponding patterns simulated from the single-crystal data (Figures S2–S4). The temperature dependence of the magnetic susceptibility  $\chi_M$  for 1–3 was measured under a 1 kOe external field and in the temperature range of 2–300 K (Figure 2). The  $\chi_M T$  value represents for one trinuclear [TM···Ln···TM] unit. The  $\chi_M T$  value of  $0.76 \text{ cm}^3 \text{ K mol}^{-1}$  at 300 K for 1 (Figure 2a) is somewhat lower than the expected value ( $1.08\text{--}1.32 \text{ cm}^3 \text{ K mol}^{-1}$ ) of two free low-spin  $\text{Fe}^{\text{III}}$  ions with a significant orbital contribution ( $[\text{Fe}^{\text{III}}]_{\text{LS}}$ ,  $S = 1/2$ ,  $g = 2.1$ , with the expected room temperature  $\chi_M T$  values in the range of  $0.54\text{--}0.68 \text{ cm}^3 \text{ K mol}^{-1}$ ) [49]. Upon cooling, the  $\chi_M T$  value decreases very slowly and reaches  $0.72 \text{ cm}^3 \text{ K mol}^{-1}$  at 2 K. In consideration of the long intra- and intermolecular Fe···Fe distances, the Fe···Fe magnetic interactions should be negligible, which is corroborated by the characteristics of the roughly invariable  $\chi_M T$  values associated with the decreasing temperature.

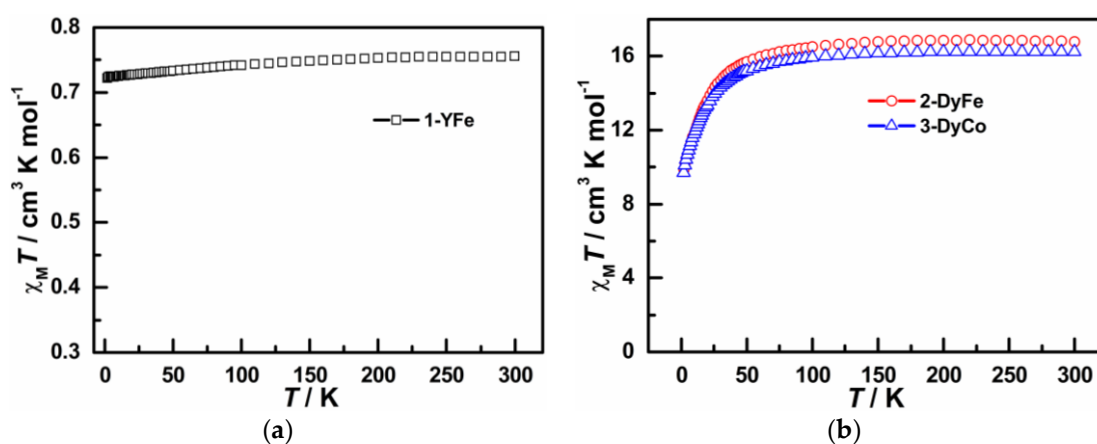


**Figure 2.** Temperature dependence of the  $\chi_M T$  products at 1 kOe dc field for compounds (a) 1; (b) 2 and 3.

At 300 K, the  $\chi_M T$  value of  $16.52 \text{ cm}^3 \text{ mol}^{-1} \text{ K}$  for 2 is a little higher than the expected value ( $15.25\text{--}15.53 \text{ cm}^3 \text{ K mol}^{-1}$ ) for one non-interacting  $\text{Dy}^{\text{III}}$  ( $14.17 \text{ cm}^3 \text{ K mol}^{-1}$ ,  $S = 5/2$ ,  $L = 5$ ,  ${}^6\text{H}_{15/2}$ ,  $J = 15/2$ ,  $g = 4/3$ ) [50] and two free  $[\text{Fe}^{\text{III}}]_{\text{LS}}$  ions. The  $\chi_M T$  value decreases gradually from 300 to about 50 K, then drops quickly to  $9.88 \text{ cm}^3 \text{ K mol}^{-1}$  at 2 K. The sustained decline of the  $\chi_M T$  value in the low-temperature region can be ascribed to the spin-orbit coupling of the two  $[\text{Fe}^{\text{III}}]_{\text{LS}}$  ions, the progressive thermal depopulation of the excited sublevels of the  ${}^6\text{H}_{15/2}$  state of the  $\text{Dy}^{\text{III}}$  ion, and the possible small magnetic interactions between the intramolecular  $\text{Dy}^{\text{III}}$  and  $[\text{Fe}^{\text{III}}]_{\text{LS}}$  ions.

The  $\chi_M T$  value of  $16.11 \text{ cm}^3 \text{ K mol}^{-1}$  at 300 K for 3 is somewhat larger than the value expected for an uncoupled  $\text{Dy}^{\text{III}}$  ion ( $14.17 \text{ cm}^3 \text{ K mol}^{-1}$ ). The temperature dependence of the  $\chi_M T$  value for 3 is typical for a monometallic  $\text{Dy}^{\text{III}}$  complex, which shows a similar gradual decrease as 2 down to 50 K and falls to  $9.71 \text{ cm}^3 \text{ K mol}^{-1}$  at 2 K. It is consistent with the large intermolecular Dy···Dy distances with the diamagnetic nature of the low-spin  $[\text{Co}(\text{CN})_5(\text{CNH}_{0.5})]^{2.5-}$  entity in mind [17,51].

The field dependence of magnetization for compounds 1 and 3 has been measured in the range of 2–15 K (Figures S5–S8). At 2 K (Figure S5), the magnetization of 1 increases gradually with the field strength, and reaches the value of  $1.43 N\beta$  with the static field up to 45 kOe, lower than the theoretical saturation value for two uncorrelated  $[\text{Fe}^{\text{III}}]_{\text{LS}}$  ions ( $2g \times S = 2 \times 2.1 \times 1/2 = 2.10 N\beta$ ). The approximate overlapping of  $M$  vs.  $H/T$  curves indicates the negligible magnetic anisotropy for the  $[\text{Fe}^{\text{III}}]_{\text{LS}}$  ions in 1 (Figure S6). For compound 3, the magnetization at 2 K increases rapidly with the increasing field at low fields and slowly at fields higher than 10 kOe, and it reaches  $7.63 N\beta$  under the highest applied experimental field of 50 kOe (Figure S7). The deviation from saturation for one isolated

Dy<sup>III</sup> ion ( $g_J \times J = 4/3 \times 15/2 = 10 N\beta$ ) indicates the presence of magnetic anisotropy and/or low-lying excited states at the Dy<sup>III</sup> ions. The non-superposition of the  $M$  vs.  $H/T$  on a single master curve confirms further the presence of magnetic anisotropy for the Dy<sup>III</sup> ions in compound **3** (Figure S8).

To probe the magnetic relaxation behavior, we measured the ac magnetic susceptibilities on the polycrystalline samples of compounds **2** and **3** under a 2 Oe ac field. As shown in Figure 3, under zero dc field, the in-phase component ( $\chi'$ ) of the ac susceptibility increases with decreasing temperature but without frequency dependence and no out-of-phase signal ( $\chi''$ ) have been detected for both compounds **2** and **3**. This phenomenon indicates that there is no magnetic relaxation in the zero dc field, which can be attributed to the QTM effect. For both compounds **2** and **3**, the coordination geometry around the Dy<sup>III</sup> ions is an axially elongated octahedron, which is not beneficial for generating strong axial anisotropy for the Dy<sup>III</sup> ions [34]. In such six-coordinate systems, the axial bond lengthening may lead to a sharp drop in the energy barrier as predicted by ab initio calculations for two-coordinate complexes of Dy<sup>III</sup> [8], and the shorter bond length in the equatorial plane leads to the introduction of the transverse field components and the enhancement of the QTM effect [40]. As a result, fast quantum tunneling and almost no magnetic relaxation exists in these compounds, which is a typical system not exhibiting the characteristics of single-ion magnet for the Dy<sup>III</sup> ions under zero dc field. In compound **2**, the influence of the small exchange interactions, between the central Dy<sup>III</sup> ion and the two terminal [Fe<sup>III</sup>]<sub>LS</sub> ions through the cyano bridges, on the single-ion magnetism of the Dy<sup>III</sup> ion could not be ignored. For compound **3**, the situation is simpler, which excludes the intramolecular Dy<sup>III</sup>...[Fe<sup>III</sup>]<sub>LS</sub> exchange interactions. In the magnetic sense, compound **3** represents the first example incorporating a magnetically isolated six-coordinate Dy<sup>III</sup> ion with a perfect  $D_{4h}$  symmetry [41].

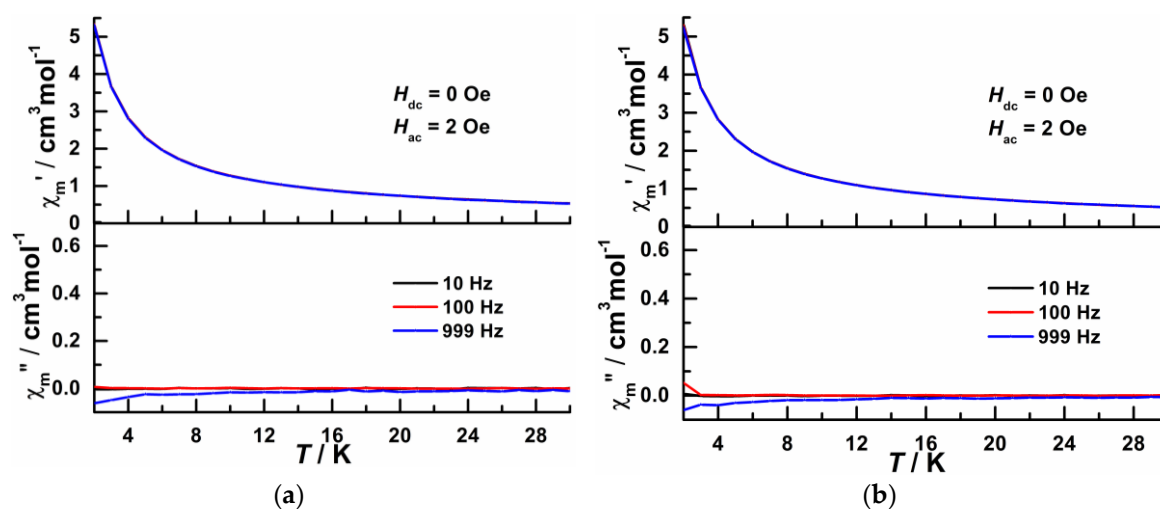


**Figure 3.** Temperature dependence of the in-phase ( $\chi'$ ) and out-of-phase ( $\chi''$ ) ac susceptibilities under a 0 Oe dc field for (a) **2** and (b) **3**.

The ac susceptibilities varying with the strength of the dc field were measured at  $f = 10, 100$  and  $999$  Hz under a 2 Oe ac field for compounds **2** and **3** to determine a certain dc field with relatively strong out-of-phase signal (Figures S9 and S10). To suppress the QTM effect, we selected a static field of 1 kOe for compound **2** (Figure 4a), 2 kOe (Figure 4b) and 3 kOe (Figure S11) for compound **3** during the measurement on the ac susceptibilities. Under the 1 kOe applied dc field for compound **2**, both  $\chi'$  and  $\chi''$  components were revealed frequency dependence without clear peaks, thus the relaxation parameters were not derived. Under both 2 kOe and 3 kOe applied dc fields for compound **3**, the  $\chi'$  components were revealed the presence of clear frequency dependence and full peaks at all measured frequencies, while the  $\chi''$  components were observed apparent frequency dependence below 4 K but the absence of well-shaped maxima in the range of frequency measured, precluding the analysis of the relaxation parameters.

The relaxation behavior of **2** and **3** under the applied fields further confirms their poor performance as a single-ion magnet of a Dy<sup>III</sup> ion with a coordination geometry of an axially elongated octahedron.

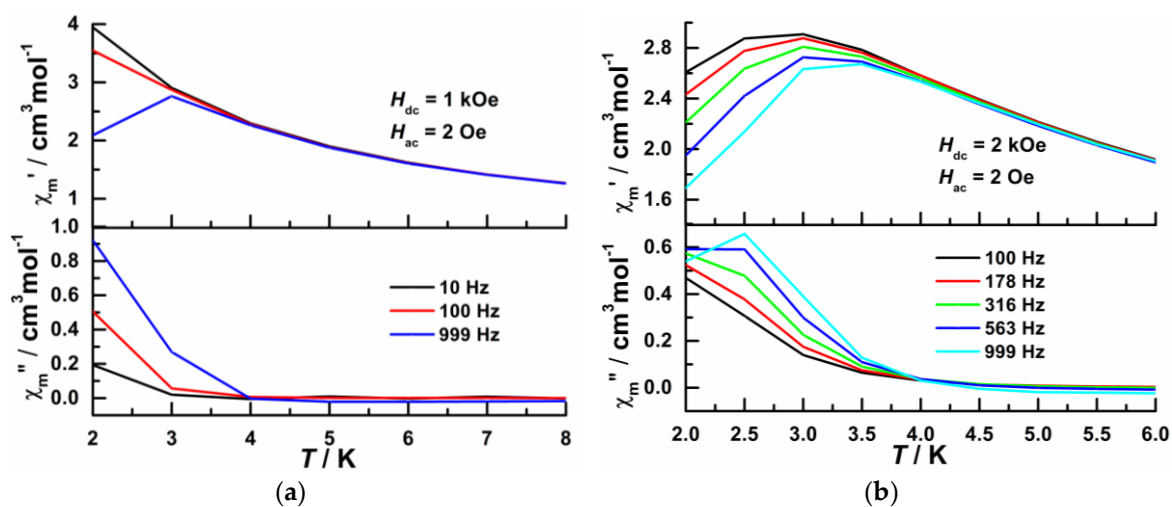


**Figure 4.** Temperature dependence of the in-phase ( $\chi'$ ) and out-of-phase ( $\chi''$ ) ac susceptibilities (a) for **2** under a 1 kOe and (b) for **3** under a 2 kOe dc field.

### 3. Experimental Section

#### 3.1. General Information

All chemicals and solvents used for synthesis were of reagent grade and used as purchased without further purification. The elemental analyses of C, H and N were performed on a Vario Micro Cube elemental analyzer (Elementar Analysensysteme GmbH, Langensfeld, Germany). Infrared (IR) spectra on powder samples obtained by crushing from crystals were recorded in the range of 4000–400  $\text{cm}^{-1}$  using KBr pellets on a Perkin Elmer Spectrum one spectrophotometer. Powder X-ray diffraction (PXRD) data for the as-prepared samples were recorded on a D8 ADVANCE (Bruker AXS, Germany) diffractometer using Cu K $\alpha$  radiation at room temperature.

#### 3.2. The preparation of Compounds 1–3

Caution! Cyanides are potentially poisonous complexes. Suitable precautions should be taken when handling them. It is of the utmost importance that all preparations be performed and stored in well-ventilated areas.

A similar procedure has been adopted to prepare compounds **1–3**.

$(\text{H}_{2.5}\text{O})_4\{\text{Y}[\text{Fe}(\text{CN})_5(\text{CNH}_{0.5})]_2(\text{HMPA})_4\}$  (**1**): Hexamethylphosphoramide (HMPA, 0.60 mmol, 0.1074 g) was added dropwise to an aqueous solution of  $\text{Y}(\text{NO}_3)_3 \cdot 6\text{H}_2\text{O}$  (0.40 mmol, 0.1532 g) and the obtained mixture was stirred for 20 min. 2.0 mL of an aqueous solution of  $\text{K}_3[\text{Fe}(\text{CN})_6]$  (0.20 mmol, 0.0658 g) was subsequently added under continuous stirring. Finally, 10 drops of HCl (1 mol/L) was added. Then the mixture was filtered and the filtrate was kept at room temperature. After a week, red block crystals were obtained. The yield (0.1036 g) was about 19.85% based on the Y<sup>III</sup> ion. Elemental analysis (%) calcd. for  $\text{C}_{36}\text{H}_{83}\text{N}_{24}\text{P}_4\text{O}_8\text{YFe}_2$ : C, 33.14; H, 6.41; N, 25.77. Found: C, 33.19; H, 5.80; N, 26.02. IR peaks (KBr,  $\text{cm}^{-1}$ ): 2942 (br), 2147 (vs), 1746 (w), 1714 (w), 1640 (w), 1487 (w), 1456 (w), 1307 (m), 1188 (m), 1121 (vs), 1068 (w), 992 (vs), 752 (m), 671 (m), 522 (w), 478 (w), 422 (w).

$(\text{H}_{2.5}\text{O})_4\{\text{Dy}[\text{Fe}(\text{CN})_5(\text{CNH}_{0.5})]_2(\text{HMPA})_4\}$  (**2**): The synthetic procedure of compound **2** was similar to compound **1**, except that  $\text{Dy}(\text{NO}_3)_3 \cdot 6\text{H}_2\text{O}$  (0.40 mmol, 0.1826 g) was used instead of  $\text{Y}(\text{NO}_3)_3 \cdot 6\text{H}_2\text{O}$ . A few days later, red block crystals were obtained. The yield (0.0808 g) was 14.66% based on the Dy<sup>III</sup> ion. Elemental analysis (%) calcd. for  $\text{C}_{36}\text{H}_{83}\text{N}_{24}\text{P}_4\text{O}_8\text{DyFe}_2$ : C, 31.37; H, 6.07; N,

24.39. Found: C, 31.27; H, 5.45; N, 24.63. IR peaks (KBr,  $\text{cm}^{-1}$ ): 3445 (br), 2943 (w), 2146 (vs), 1636 (w), 1488 (w), 1457 (w), 1308 (m), 1189 (m), 1118 (vs), 1067 (w), 992 (vs), 752 (m), 670 (w), 526 (w), 479 (w), 422 (w).

( $\text{H}_{2.5}\text{O}$ )<sub>4</sub>{Dy[Co(CN)<sub>5</sub>(CNH<sub>0.5</sub>)]<sub>2</sub>(HMPA)<sub>4</sub>} (3): Compound 3 was synthesized by the same procedure as that for compound 2 except for using  $\text{K}_3[\text{Co}(\text{CN})_6]$  (0.2 mmol, 0.0665 g) instead of  $\text{K}_3[\text{Fe}(\text{CN})_6]$ . After three days, colorless block crystals were obtained. The yield (0.0531 g) was 19.18% based on the Dy<sup>III</sup> ion. Elemental analysis (%) calcd. for  $\text{C}_{36}\text{H}_{83}\text{N}_{24}\text{P}_4\text{O}_8\text{DyCo}_2$ : C, 31.23; H, 6.04; N, 24.28. Found: C, 30.34; H, 5.61; N, 23.74. The relatively large difference in the content of the calculated and experimental carbon elements might come from the incomplete combustion of the metalocyanate during the elemental analysis experiments. IR peaks (KBr,  $\text{cm}^{-1}$ ): 3415 (br), 2935 (m), 2153 (vs), 1487 (w), 1454 (w), 1309 (m), 1189 (m), 1118 (vs), 1068 (w), 993 (vs), 750 (s), 467 (m), 423 (w).

### 3.3. X-ray Crystallography

Determination of the unit cell, data collection and reduction for compounds 1–3 were performed on a Bruker Smart APEX II CCD area detector diffractometer with graphite-monochromated Mo  $\text{K}\alpha$  radiation ( $\lambda = 0.71073 \text{ \AA}$ ). All of the diffraction data were collected at room temperature and corrected for Lorentz and polarization effects. Adsorption corrections were performed by SADABS (Bruker, 2014) method [52]. Using Olex2 [53] as the graphical interface, the structures of the three compounds were solved by direct methods of SHELXS-2008 program and refined by the full-matrix least-squares techniques based on  $F^2$  using SHELXL-2015 program [54,55]. All of the non-hydrogen atoms were refined with anisotropic thermal parameters. The protonated hydrogen atoms on the hydronium ions and the axial terminal cyano groups of the  $[\text{TM}(\text{CN})_5(\text{CNH}_{0.5})]^{2.5-}$  entities were located by difference Fourier map and refined isotropically. The other hydrogen atoms were introduced at the calculated positions and refined with isotropic thermal parameters and a fixed geometry riding on their parent atoms. The crystal data and structural refinement details of 1–3 are summarized in Table 1. The selected bond lengths and angles are listed in Tables S1–S6 in the supplementary materials.

The crystallographic data of compounds 1–3 were deposited to the Cambridge Crystallographic Data Center with Nos. CCDC 1818724–1818726. Copies of the data can be obtained free of charge via [www.ccdc.cam.ac.uk/conts/retrieving.html](http://www.ccdc.cam.ac.uk/conts/retrieving.html) (or from the Cambridge Crystallographic Data Centre, 12 Union Road, Cambridge CB2 1EZ, UK; fax: (+44) 1223-336-033; or deposit@ccdc.ca.ac.uk).

### 3.4. Magnetic Measurements

Static magnetic susceptibility measurements of 1–3 in the range 2–300 K were carried out on a Quantum Design MPMS-7 SQUID magnetometer. Alternating current susceptibilities of 1–3 were measured with an oscillating field of 2 Oe and ac frequencies in the range of 10–1000 Hz. All of the magnetic measurements were performed on the polycrystalline samples tightly packed and sealed with a capsule to avoid the anisotropic orientation. Diamagnetic corrections were made with Pascal's constants for all the constituent atoms [50].

## 4. Conclusions

Three isostructural cyano-bridged 3d–4f compounds 1, 2 and 3 have been synthesized utilizing the  $[\text{TM}(\text{CN})_5(\text{CNH}_{0.5})]^{2.5-}$  entities as bridging ligands and the highly sterically hindered HMPA as auxiliary ligands to restrict the coordination number of the lanthanide ions. The resulted linear heterotrimeric structures contain two terminal  $[\text{TM}(\text{CN})_5(\text{CNH}_{0.5})]^{2.5-}$  entities and a central six-coordinate lanthanide ion exhibiting a coordination geometry of an axially elongated octahedron with a perfect  $D_{4h}$  symmetry, which represent one kind of typical model compounds for studying the single-ion magnetic relaxation dynamics. Dynamic magnetic susceptibility measurements on compounds 2 and 3 revealed the absence of magnetic relaxation behavior under zero dc field. The weak frequency dependence of compound 3 under an applied field of 2 kOe and 3 kOe proves that the poor relaxation behavior is mainly derived from the single Dy<sup>III</sup> ion. The research suggests

that the six-coordinate Dy<sup>III</sup> ion with a coordination geometry of an axially elongated octahedron is not conducive to uniaxial magnetic anisotropy, and it is a typical system with the absence of single-ion magnetism. For other isostructural heterotrimeric structures, the magnetic relaxation dynamics of the lanthanide ion with prolate electron densities such as Er<sup>III</sup> is currently in progress.

**Supplementary Materials:** Supplementary materials are available online at <http://www.mdpi.com/2304-6740/6/2/36/s1>. cif and check cif files of compounds **1**, **2** and **3**, Table S1, S3, and S5: Selected bond lengths (Å) and angles (°) for **1–3**, Table S2, S4, and S6: Hydrogen bonding geometry for **1–3**, Table S7: Continuous shaped measures (CShM) for **1–3** using SHAPE 2.1, Figure S1: The disorder in the molecular structure of compound **2**, Figures S2–S4: Powder X-ray diffraction patterns of compound **1**, **2** and **3** for the as-synthesized samples and the simulated one, Figures S5 and S7: Field dependence of the magnetization at the temperatures of 2 K, 3 K, 5 K, 10 K, and 15 K for a polycrystalline sample of **1** and **3**, Figures S6 and S8: Plots of the reduced magnetization  $M$  vs  $H/T$  at the temperatures of 2 K, 3 K, 5 K, 10 K, and 15 K for a polycrystalline sample of **1** and **3**, Figures S9 and S10: Field dependence of the in-phase ( $\chi'$ , inset) and out-of-phase ( $\chi''$ ) ac susceptibilities for **2** and **3** with  $f = 10, 100$  and 999 Hz, Figure S11: Temperature dependence of the in-phase ( $\chi'$ ) and out-of-phase ( $\chi''$ ) ac susceptibilities for **3** under a 3 kOe dc field.

**Acknowledgments:** This work is supported by the National Natural Science Foundation of China (21201061), the State Scholarship Fund of China (201308420653), and the Scientific Research Foundation of Education Commission of Hubei Province (Q20111008).

**Author Contributions:** Wenhua Zhu conceived and designed the experiments; Xia Xiong performed the experiments; Wenhua Zhu and Xia Xiong analyzed the data; Haoling Sun contributed the magnetic measurements; Yangyu Liu, Shan Li, Anqi Xue, Juan Wang, and Chi Zhang contributed part of the analysis and discussions; Wenhua Zhu and Xia Xiong wrote the paper.

**Conflicts of Interest:** The authors declare no conflict of interest.

## References

1. Natterer, F.D.; Yang, K.; Paul, W.; Willke, P.; Choi, T.; Greber, T.; Heinrich, A.J.; Lutz, C.P. Reading and writing single-atom magnets. *Nature* **2017**, *543*, 226–228. [[CrossRef](#)] [[PubMed](#)]
2. Ishikawa, N.; Sugita, M.; Ishikawa, T.; Koshihara, S.; Kaizu, Y. Lanthanide double-decker complexes functioning as magnets at the single-molecular level. *J. Am. Chem. Soc.* **2003**, *125*, 8694–8695. [[CrossRef](#)] [[PubMed](#)]
3. Rinehart, J.D.; Long, J.R. Exploiting single-ion anisotropy in the design of f-element single-molecule magnets. *Chem. Sci.* **2011**, *2*, 2078–2085. [[CrossRef](#)]
4. Sorace, L.; Cristiano, B.C.; Gatteschi, D. Lanthanides in molecular magnetism: Old tools in a new field. *Chem. Soc. Rev.* **2011**, *40*, 3092–3104. [[CrossRef](#)] [[PubMed](#)]
5. Woodruff, D.N.; Winpenny, R.E.P.; Layfield, R.A. Lanthanide single-molecule magnets. *Chem. Rev.* **2013**, *113*, 5110–5148. [[CrossRef](#)] [[PubMed](#)]
6. Sessoli, R.; Gatteschi, D.; Caneschi, A.; Novak, M.A. Magnetic bistability in a metal-ion cluster. *Nature* **1993**, *365*, 141–143. [[CrossRef](#)]
7. Gupta, T.; Rajaraman, G. How strongly are the magnetic anisotropy and coordination numbers correlated in lanthanide based molecular magnets? *J. Chem. Sci.* **2014**, *126*, 1569–1579. [[CrossRef](#)]
8. Chilton, N.F. Design criteria for high-temperature single-molecule magnets. *Inorg. Chem.* **2015**, *54*, 2097–2099. [[CrossRef](#)] [[PubMed](#)]
9. Gregson, W.; Chilton, N.F.; Ariciu, A.; Tuna, F.; Crowe, I.F.; Lewis, W.; Blake, A.J.; Collison, D.; McInnes, E.J.L.; Winpenny, R.E.P.; et al. A monometallic lanthanide bis(methanediide) single molecule magnet with a large energy barrier and complex spin relaxation behaviour. *Chem. Sci.* **2016**, *7*, 155–165. [[CrossRef](#)]
10. Ungur, L.; Chibotaru, L.F. Magnetic anisotropy in the excited states of low symmetry lanthanide complexes. *Phys. Chem. Chem. Phys.* **2011**, *13*, 20086–20090. [[CrossRef](#)] [[PubMed](#)]
11. Chilton, N.F.; Collison, D.; McInnes, E.J.L.; Winpenny, R.E.P.; Soncini, A. An electrostatic model for the determination of magnetic anisotropy in dysprosium complexes. *Nat. Commun.* **2013**, *4*, 2551. [[CrossRef](#)] [[PubMed](#)]
12. Ganivet, C.R.; Ballesteros, B.; de la Torre, G.; Clemente-Juan, J.M.; Coronado, E.; Torres, T. Influence of peripheral substitution on the magnetic behavior of single-ion magnets based on homo- and heteroleptic Tb<sup>III</sup> bis(phthalocyaninate). *Chem. Eur. J.* **2013**, *19*, 1457–1465. [[CrossRef](#)] [[PubMed](#)]

13. Liu, J.L.; Chen, Y.C.; Zheng, Y.Z.; Lin, W.Q.; Ungur, L.; Wernsdorfer, W.; Chibotaru, L.F.; Tong, M.L. Switching the anisotropy barrier of a single-ion magnet by symmetry change from quasi- $D_{5h}$  to quasi- $O_h$ . *Chem. Sci.* **2013**, *4*, 3310–3316. [[CrossRef](#)]
14. Chen, Y.C.; Liu, J.L.; Ungur, L.; Liu, J.; Li, Q.W.; Wang, L.F.; Ni, Z.P.; Chibotaru, L.F.; Chen, X.M.; Tong, M.L. Symmetry-supported magnetic blocking at 20 K in pentagonal bipyramidal Dy(III) single-ion magnets. *J. Am. Chem. Soc.* **2016**, *138*, 2829–2837. [[CrossRef](#)] [[PubMed](#)]
15. Gupta, S.K.; Rajeshkumar, T.; Rajaraman, G.; Murugavel, R. An air-stable Dy(III) single-ion magnet with high anisotropy barrier and blocking temperature. *Chem. Sci.* **2016**, *7*, 5181–5191. [[CrossRef](#)]
16. Ding, Y.S.; Chilton, N.F.; Winpenny, R.E.P.; Zheng, Y.Z. On approaching the limit of molecular magnetic anisotropy: A near-perfect pentagonal bipyramidal dysprosium(III) single-molecule magnet. *Angew. Chem. Int. Ed.* **2016**, *55*, 16071–16074. [[CrossRef](#)] [[PubMed](#)]
17. Zhang, Y.; Guo, Z.; Xie, S.; Li, H.L.; Zhu, W.H.; Liu, L.; Dong, X.Q.; He, W.X.; Ren, J.C.; Liu, L.Z.; et al. Tuning the origin of magnetic relaxation by substituting the 3d or rare-earth ions into three isostructural cyano-bridged 3d–4f heterodinuclear compounds. *Inorg. Chem.* **2015**, *54*, 10316–10322. [[CrossRef](#)] [[PubMed](#)]
18. Guo, F.S.; Day, B.M.; Chen, Y.C.; Tong, M.L.; Mansikkam-ki, A.; Layfield, R.A. A dysprosium metallocene single-molecule magnet functioning at the axial limit. *Angew. Chem. Int. Ed.* **2017**, *56*, 11445–11449. [[CrossRef](#)] [[PubMed](#)]
19. Goodwin, C.A.P.; Ortu, F.; Reta, D.; Chilton, N.F.; Mills, D.P. Molecular magnetic hysteresis at 60 kelvin in dysprosocenium. *Nature* **2017**, *548*, 439–442. [[CrossRef](#)] [[PubMed](#)]
20. Blagg, R.J.; Ungur, L.; Tuna, F.; Speak, J.; Comar, P.; Collison, D.; Wernsdorfer, W.; McInnes, E.J.L.; Chibotaru, L.; Winpenny, R.E.P. Magnetic relaxation pathways in lanthanide single-molecule magnets. *Nat. Chem.* **2013**, *5*, 673–678. [[CrossRef](#)] [[PubMed](#)]
21. Chilton, N.F.; Goodwin, C.A.P.; Mills, D.P.; Winpenny, R.E.P. The first near-linear bis(amide) f-block complex: A blueprint for a high temperature single molecule magnet. *Chem. Commun.* **2015**, *51*, 101–103. [[CrossRef](#)] [[PubMed](#)]
22. Zhang, P.; Zhang, L.; Wang, C.; Xue, S.F.; Lin, S.Y.; Tang, J.K. Equatorially coordinated lanthanide single ion magnets. *J. Am. Chem. Soc.* **2014**, *136*, 4484–4487. [[CrossRef](#)] [[PubMed](#)]
23. Zhang, P.; Jung, J.; Zhang, L.; Tang, J.K.; Guennic, B.L. Elucidating the magnetic anisotropy and relaxation dynamics of low-coordinate lanthanide compounds. *Inorg. Chem.* **2016**, *55*, 1905–1911. [[CrossRef](#)] [[PubMed](#)]
24. Xiong, J.; Ding, H.Y.; Meng, Y.S.; Gao, C.; Zhang, X.J.; Meng, Z.S.; Zhang, Y.Q.; Shi, W.; Wang, B.W.; Gao, S. Hydroxide-bridged five-coordinate Dy<sup>III</sup> single-molecule magnet exhibiting the record thermal relaxation barrier of magnetization among lanthanide-only dimers. *Chem. Sci.* **2017**, *8*, 1288–1294. [[CrossRef](#)] [[PubMed](#)]
25. Liu, S.S.; Meng, Y.S.; Zhang, Y.Q.; Meng, Z.S.; Lang, K.; Zhu, Z.L.; Shang, C.F.; Wang, B.W.; Gao, S. A six-coordinate dysprosium single-ion magnet with trigonal-prismatic geometry. *Inorg. Chem.* **2017**, *56*, 7320–7323. [[CrossRef](#)] [[PubMed](#)]
26. Woodruff, D.N.; Tuna, F.; Bodensteiner, M.; Winpenny, R.E.P.; Layfield, R.A. Single-molecule magnetism in tetrametallic terbium and dysprosium thiolate cages. *Organometallics* **2013**, *32*, 1224–1229. [[CrossRef](#)]
27. Blagg, R.J.; Murny, C.A.; McInnes, E.J.L.; Tuna, F.; Winpenny, R.E.P. Single pyramid magnets: Dy<sup>5</sup> pyramids with slow magnetic relaxation to 40 K. *Angew. Chem. Int. Ed.* **2011**, *50*, 6530–6533. [[CrossRef](#)] [[PubMed](#)]
28. Norel, L.; Darago, L.E.; Guennic, B.L.; Chakarawet, K.; Gonzalez, M.I.; Olshansky, J.H.; Rigaut, S.; Long, J.R. A terminal fluoride ligand generates highly axial magnetic anisotropy in dysprosium complexes. *Angew. Chem. Int. Ed.* **2018**, *130*, 1951–1956. [[CrossRef](#)]
29. Yao, M.X.; Zhu, Z.X.; Lu, X.Y.; Deng, X.W.; Jing, S. Rare single-molecule magnets with six-coordinate Ln<sup>III</sup> ions exhibiting a trigonal antiprism configuration. *Dalton Trans.* **2016**, *45*, 10689–10695. [[CrossRef](#)] [[PubMed](#)]
30. Latendresse, T.P.; Bhuvanesh, N.S.; Nippe, M. Slow magnetic relaxation in a lanthanide-[1]metallocenophane complex. *J. Am. Chem. Soc.* **2017**, *139*, 8058–8061. [[CrossRef](#)] [[PubMed](#)]
31. Na, B.; Zhang, X.J.; Shi, W.; Zhang, Y.Q.; Wang, B.W.; Gao, C.; Gao, S.; Cheng, P. Six-coordinate lanthanide complexes: Slow relaxation of magnetization in the dysprosium(III) complex. *Chem. Eur. J.* **2014**, *20*, 15975–15980. [[CrossRef](#)] [[PubMed](#)]
32. Efthymiou, C.G.; Stamatatos, T.C.; Papatriantafyllopoulou, C.; Tasiopoulos, A.J.; Wernsdorfer, W.; Perlepes, S.P.; Christou, G. Nickel/lanthanide single-molecule magnets: {Ni<sub>3</sub>Ln} “stars” with a ligand derived from the metal-promoted reduction of di-2-pyridyl ketone under solvothermal conditions. *Inorg. Chem.* **2010**, *49*, 9737–9739. [[CrossRef](#)] [[PubMed](#)]

33. Meihaus, K.R.; Rinehart, J.D.; Long, J.R. Dilution-induced slow magnetic relaxation and anomalous hysteresis in trigonal prismatic dysprosium(III) and uranium(III) complexes. *Inorg. Chem.* **2011**, *50*, 8484–8489. [[CrossRef](#)] [[PubMed](#)]
34. König, S.N.; Chilton, N.F.; Maichle-Mössner, C.; Pineda, E.M.; Pugh, T.; Anwander, R.; Layfield, R.A. Fast magnetic relaxation in an octahedral dysprosium tetramethyl-aluminate complex. *Dalton Trans.* **2014**, *43*, 3035–3038. [[CrossRef](#)] [[PubMed](#)]
35. Meihaus, K.R.; Minasian, S.G.; Lukens, W.W., Jr.; Kozimor, S.A.; Shun, D.K.; Tyliczack, T.; Long, J.R. Influence of pyrazolate vs *N*-heterocyclic carbene ligands on the slow magnetic relaxation of homoleptic trischelate lanthanide(III) and uranium(III) complexes. *J. Am. Chem. Soc.* **2014**, *136*, 6056–6058. [[CrossRef](#)] [[PubMed](#)]
36. Singh, S.K.; Beg, M.F.; Rajaraman, G. Role of magnetic exchange interactions in the magnetization relaxation of {3d–4f} single-molecule magnets: A theoretical perspective. *Chem. Eur. J.* **2016**, *22*, 672–680. [[CrossRef](#)] [[PubMed](#)]
37. Janzen, D.E.; Juchum, M.; Presow, S.R.; Ronson, T.K.; Mohr, W.; Clérac, R.; Feltham, H.L.C.; Brooker, S. Trigonal (–3) symmetry octahedral lanthanide(III) complexes of zwitterionic tripodal ligands: Luminescence and magnetism. *Supramol. Chem.* **2016**, *28*, 125–140. [[CrossRef](#)]
38. Klementyeva, S.V.; Afonin, M.Y.; Bogomyakov, A.S.; Gamer, M.T.; Roesky, P.W.; Konchenko, S.N. Mono- and dinuclear rare-earth chlorides ligated by a mesityl-substituted  $\beta$ -diketiminato. *Eur. J. Inorg. Chem.* **2016**, *22*, 3666–3672. [[CrossRef](#)]
39. Lim, K.S.; Baldovi, J.J.; Jiang, S.D.; Koo, B.H.; Kang, D.W.; Lee, W.R.; Koh, E.K.; Gaita-Ariño, A.; Coronado, E.; Slota, M.; et al. Custom coordination environments for lanthanoids: Tripodal ligands achieve near-perfect octahedral coordination for two dysprosium-based molecular nanomagnets. *Inorg. Chem.* **2017**, *56*, 4911–4917. [[CrossRef](#)] [[PubMed](#)]
40. Liu, M.J.; Yuan, J.; Zhang, Y.Q.; Sun, H.L.; Liu, C.M.; Kou, H.Z. Chiral six-coordinate Dy(III) and Tb(III) complexes of an achiral ligand: Structure, fluorescence, and magnetism. *Dalton Trans.* **2017**, *46*, 13035–13042. [[CrossRef](#)] [[PubMed](#)]
41. Zeng, D.; Ren, M.; Bao, S.S.; Li, L.; Zheng, L.M. A luminescent heptanuclear Dy<sub>7</sub> complex showing field-induced slow magnetization relaxation. *Chem. Commun.* **2014**, *50*, 8356–8359. [[CrossRef](#)] [[PubMed](#)]
42. Tiron, R.; Wernsdorfer, W.; Tuyeras, F.; Sculler, A.; Marvaud, V.; Verdaguer, M. Hexacyanometalate molecular chemistry: Trinuclear CrNi<sub>2</sub> complexes; micro-SQUID magnetisation studies of intermolecular interactions. *Polyhedron* **2003**, *22*, 2427–2433. [[CrossRef](#)]
43. Parker, R.J.; Lu, L.D.; Batten, S.R.; Moubaraki, B.; Murray, K.S.; Spiccia, L.; Cashion, J.D.; David Rae, A.; Willis, A.C. Synthesis, crystal structures and magnetic properties of linear and bent trinuclear complexes formed by hexacyanometalates and copper(II) complexes. *J. Chem. Soc. Dalton Trans.* **2002**, 3723–3730. [[CrossRef](#)]
44. Tanaka, R.; Okazawa, A.; Konaka, H.; Sasaki, A.; Kojima, N.; Matsushita, N. Unique Hydration/dehydration-induced vapochromic behavior of a charge-transfer salt comprising viologen and hexacyanidoferrate(II). *Inorg. Chem.* **2018**, *57*, 2209–2217. [[CrossRef](#)] [[PubMed](#)]
45. Bar, E.; Fuchs, J.; Rieger, D.; Aguilar-Parrilla, F.; Limbach, H.; Fehlhämmer, W.P. Molecular and ionic hydrogen isocyanide (CNH) adducts with N–H···O– and “super-short” N–H···N– hydrogen bridges: Metal-stabilized hydrogen bisisocyanides. *Angew. Chem. Int. Ed.* **1991**, *30*, 88–90. [[CrossRef](#)]
46. Lluell, M.; Casanova, D.; Cirera, J.; Bofill, J.M.; Alemany, P.; Alvarez, S. *SHAPE*; (Version 2.1); Universitat de Barcelona: Barcelona, Spain, 2013.
47. Casanova, D.; Alemany, P.; Bofill, J.M.; Alvarez, S. Shape and symmetry of heptacoordinate transition-metal complexes: Structural trends. *Chem. Eur. J.* **2003**, *9*, 1281–1285. [[CrossRef](#)] [[PubMed](#)]
48. Haser, R.; Bonnet, B.; Roziere, J. Caractéristiques spectroscopiques des liaisons hydrogène N–H–N très fortes. Études des acides A<sub>3</sub>(CN)<sub>6</sub>, (A = H, D; M = Fe, Co) par spectroscopie de vibration. *J. Mol. Struct.* **1977**, *40*, 177–189. [[CrossRef](#)]
49. Visinescu, D.; Toma, L.M.; Fabelo, O.; Ruiz-Pérez, C.; Lloret, F.; Julve, M. Low-dimensional 3d–4f complexes assembled by low-spin [Fe<sup>III</sup>(phen)(CN)<sub>4</sub>]<sup>–</sup> anions. *Inorg. Chem.* **2013**, *52*, 1525–1537. [[CrossRef](#)] [[PubMed](#)]
50. Kahn, O. *Molecular Magnetism*; VCH Publishers: New York, NY, USA, 1993; ISBN 1-56081-566-3.
51. Costes, J.P.; Dahan, F.; Dupuis, A.; Laurent, J.P. Nature of the magnetic interaction in the (Cu<sup>2+</sup>, Ln<sup>3+</sup>) pairs: An empirical approach based on the comparison between homologous (Cu<sup>2+</sup>, Ln<sup>3+</sup>) and (Ni<sub>1S</sub><sup>2+</sup>, Ln<sup>3+</sup>) complexes. *Chem. Eur. J.* **1998**, *4*, 1616–1620. [[CrossRef](#)]

52. Sheldrick, G.M. *SADABS*; Program for Siemens Area Detector Absorption Correction; University of Göttingen: Göttingen, Germany, 1996.
53. Dolomanov, O.V.; Bourhis, L.J.; Gildea, R.J.; Howard, J.A.K.; Puschmann, H. *OLEX2*: A complete structure solution, refinement and analysis program. *J. Appl. Crystallogr.* **2009**, *42*, 339–341. [[CrossRef](#)]
54. Sheldrick, G.M. *SHELXS97*; Program for the Solution of Crystal Structures; University of Göttingen: Göttingen, Germany, 1997.
55. Sheldrick, G.M. A short history of SHELX. *Acta Crystallogr. Sect. A Fund. Crystallogr.* **2008**, *A64*, 112–122. [[CrossRef](#)] [[PubMed](#)]



© 2018 by the authors. Licensee MDPI, Basel, Switzerland. This article is an open access article distributed under the terms and conditions of the Creative Commons Attribution (CC BY) license (<http://creativecommons.org/licenses/by/4.0/>).